Hybrid fuzzy logic and gravitational search algorithm-based multiple filters for image restoration

A. Senthilselvi*

Department of Computer Science and Engineering,
Sethu Institute of Technology,
Virudhunagar, India
Email: senthilselvi0384@gmail.com
*Corresponding author

R. Sukumar

Department of Computer Science and Engineering,
School of Engineering and Technology,
Jain University,
JGI Global Campus,
Jakkasandra post, Kanakapura Taluk, Karnataka, India
Email: rsugumdevi@rediffmail.com

S. Senthilpandi

Department of Information Technology,
Sethu Institute of Technology,
Virudhunagar, India
Email: Mailtosenthil.ks@gmail.com

Abstract: In this paper, we present a multiple image filters for removal of impulse noises from test images. It utilises fuzzy logic (FL) approach to design a noise detector (ND) optimised by gravitational search algorithm (GSA) and utilises median filter (MF) for restoring. The proposed multiple filters used the FL approach to detect each pixels of a tests image are noise corrupted or not. If it is considered as noise-corrupted, the multiple filters restore it with the MF filter. Otherwise, it remains unchanged. We split the image into number of windows and each window apply the multiple filters. The filter output is used for the rule generation. The optimal rules are selected using GSA and given to the fuzzy logic system to detect the noise pixel. The experimental results are carried out using different noise level and different methods. The performance measured in terms of PSNR, MSE and visual quality.

Keywords: image restoration; impulse noise; fuzzy logic; multiple filters; median filter; standard test images; gravitational search algorithm; GSA.

Reference to this paper should be made as follows: Senthilselvi, A., Sukumar, R. and Senthilpandi, S. (2020) 'Hybrid fuzzy logic and gravitational search algorithm-based multiple filters for image restoration', *Int. J. Data Analysis Techniques and Strategies*, Vol. 12, No. 1, pp.76–97.

Biographical notes: A. Senthilselvi is an Assistant Professor of Computer Science and Engineering in Sethu Institute of Technology, Virudhunagar. She received her BE degree in Electronics and Communication Engineering from Anna University, Tamilnadu, India in 2005. She received her MTech degree in Information Technology from Kalasalingam University, Tamilnadu, India in 2010. She is currently pursuing her PhD degree.

R. Sukumar is a Professor of Computer Science and Engineering in Kalaigar Karunanidhi Institute of Technology, Coimbatore. He received his BE degree in Electronics and Communication Engineering from Madurai Kamaraj University, Tamilnadu, India in 1992. He received his ME degree in Computer Science and Engineering from Manonmaniam Sundaranar University, Tirunelveli, Tamilnadu, India in 2005. He received his PhD degree from Anna University Chennai, Tamilnadu, India in 2010. His research interests include cryptography and Network Security and he has published more than ten papers in reputed international journals.

S. Senthilpandi is an Assistant Professor of Information Technology in Sethu Institute of Technology, Virudhunagar. He received his BTech degree in Information Technology from Anna University, Tamilnadu, India in 2006. He received his MTech degree in Information Technology from Kalasalingam University, Tamilnadu, India in 2010. He is currently pursuing her PhD degree.

1 Introduction

Image restoration is one of the most important and fundamental issues in image processing. It has been widely used in various fields, such as computer vision, medical imaging, etc. (Mei and Huang, 2016). Image restoration attempts to reconstruct or recover an image that has been degraded by using a priori knowledge of the degradation phenomenon. Thus, restoration techniques focus on modelling the degradation and applying the inverse model in order to recover a de-noised image (Mbarki et al., 2016). Similarly, image de-noising, which is a common procedure in digital image processing, aims to reduce noise from images (Sakthidasan and Nagappanb, 2016). Various de-noising image filters are used for reducing noise from images. In general, filtering procedures consist of the following two steps:

1 an impulse detector classifies the input pixels as either noise-corrupted or noise-free

2 a noise reduction filter modifies only those pixels that are classified as noise-corrupted.

Low power, less area, and high speed are key factors considered for designing an efficient filter. A filter with lower evaluation time (ET) is better than a filter with higher ET when other performance measures are constant (Zhao and Feng, 2012).

The purpose of image restoration is to ‘compensate for’ or ‘undo’ defects that degrade an image. Degradation comes in many forms, including motion blur, noise, and camera misfocus. In cases like motion blur, it is possible to obtain a very good estimate of the actual blurring function and ‘undo’ the blur to restore the original image (Chan et al., 2005). However, in cases where the image is corrupted by noise, the best way can hope to achieve is to compensate for the resulting degradation. Owing to the ill-posed

nature of image restoration, an image restoration solution is generally not unique. To find a better solution, prior knowledge of images can be used to regularise the image restoration problem (Lukac and Plataniotis, 2007). One of the most commonly used regularisation models is the total variation (TV) model (Molina et al., 2006). Images can be contaminated (Rao, 2006) with different types of noise, for different reasons. For example, noise can occur because of the circumstances of recording, transmission, or storage, copying, scanning, etc. Impulse noise and additive noise are most commonly found. It is a great challenge to develop algorithms that can remove noise from the image without disturbing its content.

Image restoration is a fundamental task in image processing. In various applications of computer vision, image processing is usually started by removing or reducing noise and other distortions from the image taken by a digital camera or obtained using some other method, for example, ultrasound scan or computer tomography (Majava, 2001). After this, the aim is to identify different segments of the image for further treatment, such as recognition and classification. In such applications, it is essential that the restoration process preserves edges since they define the location of different segments and objects in an image (Arridge, 1999). Image restoration techniques are utilised, among many other fields, in telecommunications and medical imaging (Kaipio et al., 2000), where measured signals and images often contain measurement and quantisation errors, i.e., noise. Noise reduction is in many cases a necessity because all classical edge detection or segmentation methods rely on derivatives to some extent (Li and Santosa, 1996; Mignotte, 2005). However, the problem of numerical differentiation is ill-posed in the sense that small perturbations in the function (surface) to be differentiated may lead to large errors in the computed derivative (Guerrero-Colon et al., 2007; Portilla and Simoncelli, 2003). Hence, the derivatives of noisy images do not contain correct information and can thus be useless as such for edge detection or segmentation purposes.

In this paper, we propose an optimal fuzzy logic (FL) with multiple filters-based impulse noise removal from test images. In this proposed work, mainly we implement two stages, first one is optimal rule generation using GSA. Another one is designing a fuzzy logic system (FLS) for noise detection and restoration. Here, at first, we split the test images into n number of window. Then each window we apply the median filter (MF) and mean filter (MNF) to obtain the distance vector. After that, we design the FLS for noise detection purpose with the help of distance vector and GSA. Finally, we find if any of the pixels is corrupted then, we replace the pixel using MF. The main objective of the proposed method is given below.

The main objective of this research is to remove the impulse noise from the test images using a combination of optimal FLS and multiple filters. The novel image restoration system is designed by two significant stages. In the first stage, an optimal rule selection procedure is developed to find optimal rule in FLS. In the second stage, based on the rule, FLS is developed which is used to detect any pixels with noises.

The remaining of the paper is arranged as follows: Section 2 explains about associated paper works and discussion. Section 3 shows the background of proposed image restoration approach and Section 4 explains about proposed image restoration approach. The experimental results are discussed in Section 5 and conclusion part is explained in Section 6.

2 Related works

In the literature survey, several methods have been proposed for image restoration in image processing. Image restoration is the practice of removing or reducing the degradation (Senthilselvi and Sukumar, 2018). Knowledge of degradation is need for successful restoration (Senthilselvi and Sukumar, 2014). Among the most recently published works are those presented as follows: Liu et al. (2016) have examined image restoration approach using a joint sparse representation in 3D-transform domain, the proposed JSR was able to represent image more sparsely and more precisely in the transform domain by performing 3D transform on each set of similar blocks. In addition to that, in order to overcome the issues of defective block matching and spurious artefact in the 3D sparse representation, JSR introduces a new nonlocal regularisation term which characterises the statistics of the nonlocal image to improve the accuracy of the estimated coefficients. The parameters of regularisation terms were calculated based on Bayesian philosophy, and a split Bregman-based technique was developed to obtain the solution in a tractable and robust manner. Moreover, Laghrib et al. (2016) have explained a multi-frame super-resolution using diffusion registration and a nonlocal variational image restoration, method consists of a non-parametric image registration based on diffusion regularisation and a nonlocal Laplace regulariser combined with a bilateral filter (BTV) in the reconstruction step to remove noise and motion outliers. The diffusion registration was employed to handle the small deformation between the unregistered images, while the combination of nonlocal Laplace and BTV was used to increase the robustness of the restoration step with respect to the blurring effect and to the noise. And also prove the existence of a solution to the well-posed registration problem. Simulation results using different images show the effectiveness and robustness of our algorithm against noise and outliers compared to other existing methods.

Rather than, Li et al. (2016) have introduced simultaneous tumour segmentation, image restoration, and blur kernel estimation in PET using multiple regularisations, the proposed method integrated TV semi-blind deconvolution and Mumford-Shah segmentation with multiple regularisations. Unlike many existing energy minimisation methods using either TV or L2 regularisation, the proposed method employed TV regularisation over tumour edges to preserve edge information, and L2 regularisation inside tumour regions to preserve the smooth change of the metabolic uptake in a PET image. The blur kernel was modelled as anisotropic Gaussian to address the resolution difference in transverse and axial directions commonly seen in a clinic PET scanner. The energy functional was rephrased using the Γ-convergence approximation and was iteratively optimised using the alternating minimisation (AM) algorithm. Furthermore, Shi et al. (2016) have explained TV image restoration using hyper-Laplacian prior with overlapping group sparsity, adopt the alternating direction method of multipliers (ADMM) method to optimise the object function of the proposed model and discuss the parameter selection criterion in the complex formulation. Finally, carry out experiments on various degrade images and compare the method with several classical state-of-the-art methods. Experimental results show that method has good performance in convergence and suppressing staircase artefacts, which makes a good balance between alleviating staircase effects and preserving image details.

Moreover, Ketter (2016) have introduced destination image restoration on facebook, have shed light on the role of Facebook as a mean of image restoration and on its unique characteristics as a multi-functional tool that can be used to address diverse audiences, to conduct both formal and informal interactions, to post various kinds of information, to bypass the news media and to serve as an additional distribution channel. Rather than others, Chen et al. (2016) examined FIRT: Filtered iterative reconstruction technique with information restoration, electron tomography by combining the algebra reconstruction technique (ART) and the nonlinear diffusion (ND) filter technique. Using both simulated and experimental data, in comparison to ART and weight back projection method, proved that FIRT could generate a better reconstruction with reduced ray artefacts and significantly improved correlation with the ground truth and partially restore the information at the non-sampled angular region, which was proved by investigating the 90° re-projection and by the cross-validation method (Johnson and Sofer, 2000). This new algorithm will be subsequently useful in the future for both cellular and molecular ET with better quality and improved structural details. Moreover, Cai et al. (2006) have presented a wavelet frame-based image restoration method. It gauges both the image to be restored and its peculiarity set.

3 Background of the proposed image restoration approach

In this section, first, we discuss the background of the GSA, the FLS and review of de-noising filters. Then the detailed of the proposed image restoration methodology will be presented.

3.1 Gravitational search algorithm

The GSA is based on Newton's gravitational force behaviour, which was proposed by Rashedi. In this algorithm, agents are considered as samples and their performance is measured by their masses. Every one of these samples attracts each other by the gravity force, and this force causes a global movement of all samples towards the samples with heavier masses. Henceforth, masses cooperate utilising a direct form of communication, through gravitational force. In GSA, each mass (agent) has four specifications: first one is the position, second one is the inertial mass, next active gravitational mass and final one is the passive gravitational mass. Each solution gravitational, inertial mass are calculated using fitness function (Adjeroh et al., 2006).

For GSA optimisation, at first, considers the N agents. The position of the i^{th} agent is defined as:

$$Y_i = \left(y_i^1, \ldots, y_i^d, \ldots, y_i^n\right) \quad \text{for } i = 1,\ 2,\ N \tag{1}$$

where y_i^d is the current position of the i^{th} agent in the d^{th} dimension, and n is the dimension of search space.

Figure 1 Flow chart of GSA (see online version for colours)

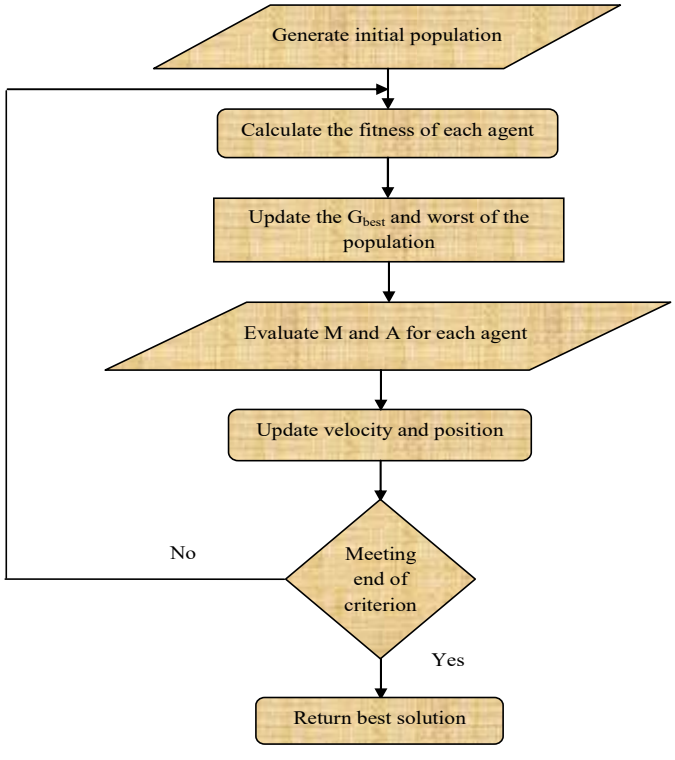

The force of the mass i from mass j is calculated based on equation (2).

$$F_{ij}^{d} = G(k)\frac{M_{pi}(k)\times M_{aj(k)}}{R_{ij}+\in}\left(y_j^d(k)-y_i^d(k)\right) \tag{2}$$

$$R_{ij}=\left\|Y_i(k).Y_j(k)\right\| \tag{3}$$

where

M_{aj} represents active gravitational mass of agent j

M_{pi} represents passive gravitational mass of agent i

$G(k)$ represents is gravitational constant at time t

$\in$ represents small constant.

R_{ij} represents Euclidian distance between two agents i and j.

Then calculate the total force acting on mass i in the d^{th} dimension in time k is given as follows:

$$F_i^d(k) = \sum_{j\in kbest,\, j\neq i} rand_j F_{ij}^d(k) \tag{4}$$

where $rand_j$ is a random number in the interval [0, 1], Kbest is the set best k fitness solution. The acceleration related to mass i in time k in the d^{th} dimension is given as follows:

$$A_i^d = \frac{F_i^d(k)}{M_{ii}(k)} \tag{5}$$

where M_{ii} is the inertial mass of i^{th} agent.

The next velocity of an agent could be calculated as a fraction of its current velocity added to its acceleration. Position and velocity of agent is calculated as follows:

$$v_i^d(k+1) = rand_i \; v_i^d(k) + A_i^d(k) \tag{6}$$

$$y_i^d(k+1) = x_i^d(k) + v_i^d(k+1) \tag{7}$$

where $rand_i$ is a uniform random variable in the interval [0, 1].

3.2 Fuzzy logic system

A FLS is utilised to design an impulse noise detector (ND) for enhancing the restoration performance of the traditional detector. Fundamentally, the fuzzy framework contains the fuzzifier, the fuzzy rule data base, the fuzzy inference engine and the de-fuzzier. The fuzzifier changes over a contribution to its relating fuzzy set. The fuzzy rule data base contains different fuzzy rules which show up in IF-THEN arrangement. The fuzzy inference engine first evaluates the fuzzy degrees of each fuzzy rule. And after that it delivers the fuzzy results of each fluffy rule. The de-fuzzifier changes over the above fuzzy set into a crisp value through utilising, for instance, the gravity strategy or the centroid technique (Lukac and Smolka, 2003). A membership function (MF) is a bend that characterises how each point in the information space is mapped to a membership value in the vicinity of 0 and 1. Contrasted with the conventional set, the membership degrees of the components in the fuzzy set can be controlled by MF, for example, trapezoidal and triangular, and so on. Nowadays, FLS is used for lot of application such as pattern recognition, decision analysis, and image filtering. In this paper, the FLS is checked whether each pixel vector in an image it is corrupted or not. The structure of FLS is given in Figure 2.

Figure 2 Fuzzy logic system (see online version for colours)

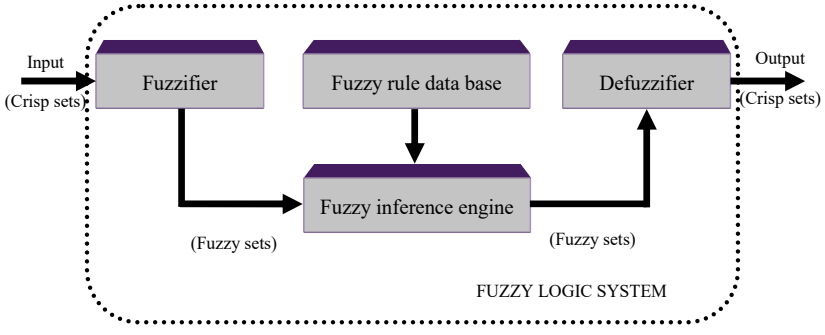

3.3 Review of image de-noising filters

3.3.1 Median filter

MF is a nonlinear technique used to remove noise from images. It is generally utilised as it is extremely compelling at removing noise while saving edges. It is especially viable at expelling impulse noise. The MF works by travelling through the image pixel by pixel replacing each value with the median value of neighbouring pixels. The median is calculated by first sorting all the pixel values from the window into numerical request, and afterward replacing the pixel being considered with the middle (median) pixel value. Let $w_{ij} = (y_1, y_2,\ldots, y_n)$ be an input of the MF. Subsequently, y_1, $y_2\ldots$ and y_n are sorted by the ascending sequence based on the pixel values $y_1 < y_2 < \ldots < y_n$. Finally, the median value of the vector is selected and which is placed in the center pixel vector. The output of the MF for the centre pixel vector w_{ij} denotes O_{MFij}.

3.3.2 Mean filter

The mean filter is a straightforward sliding-window spatial filter. This filter is used to replaces the centre value in the window with the average (mean) of all the pixel values in the window. The window is usually square but can be any shape. Let $w_{ij} = (y_1, y_2, \ldots, y_n)$ be an input of the mean filter. Subsequently, we take the average of window and replace the centre pixel x_{ij} into average value of window w_{ij}. The output of the mean filter for the centre pixel vector *wij* denotes O_{Mij}.

4 Proposed image restoration methodology

Image restoration is one of the most important and fundamental issues in image processing. It has been widely used in various fields, such as computer vision, medical imaging, etc. The main aim of image restoration is to remove the noise present in the noisy image. Like that, main objective of proposed methodology is to restore the test image based on multiplefilter and optimal FLS. This paper presents a multiple image filter for the removal of impulse noises present intest images. Moreover, the proposed system employs FL technique to design a ND optimised by GSA and utilises MF for restoring. The proposed image restoration methodology is given in Figure 3.

Figure 3 shows the block diagram of proposed image restoration approach. Consider the noisy image $I(i, j)$ size of $M \times N$ which has some of the impulse noise. To remove the noise present in the input image and restore the image is the main objective of proposed methodology. Here, at first, we split the image into n number of windows w_{ij}. For each window w_{ij}, we apply the MF, and mean filter (MNF). Here, we obtain the output of $Y_{MF,ij}$ and $Y_{MN,ij}$. Then, we calculate the difference between $Y_{MF,ij}$ and $Y_{MN,ij}$ with noisy window w_{ij}. Here, we obtain the distance vector d_{MFij}, and d_{Mij}. These two distance vectors (d_{MFij}, and d_{Mij}) are given to the input of the FLS. Based on these two values, the system detects current pixel is noise corrupted or not using the optimal FLS. If it is considered as noise-corrupted, the multiple filters restore it with the MF filter. Otherwise, it remains unchanged. Finally, we obtain the noise free image.

Figure 3 Overall concept of proposed image restoration (see online version for colours)

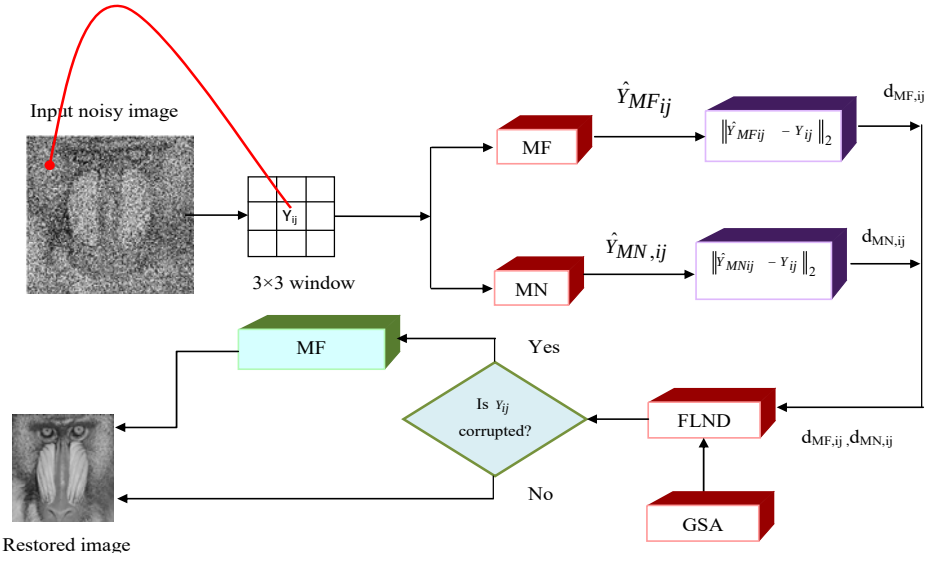

4.1 FL-based ND

In this proposed work, fuzzy logic noise detector (FLND) system performs a ND, which employs the FL technique to judge the central pixel vector Y_{ij} in the filter window W_{ij} where it is corrupted or not. The proposed FLND system first utilises the MF and mean filter to judge Y_{ij} of W_{ij} in $I(i, j)$ using various filter windows with different sizes. Two vectors $Y_{MF,ij}$ and $Y_{MN,ij}$ represents the restoration results of using the MF, and the mean filter (MNF), respectively, while feeding w_{ij} into them. Moreover, $d_{MF,ij}$, and $d_{MN,ij}$ represents the distances between noisy window w_{ij} with $Y_{MF,ij}$, and $Y_{MN,ij}$, respectively. The inputs of the FLND consist of two distances $d_{MF,ij}$, and $d_{MN,ij}$. Note that it plays a role of a binary classifier here. That is, it maps an input vector ($d_{MFij,}$ and d_{Mij}) to {0, 1}. Like that, we generate the distance vector for all the pixels present in the input image. Then, based on the distance vector we generate the rule for the FLS. The optimalnumber of rules is used to increase the system accuracy and reduce the training time of the system. Optimal rule generation process is explained below.

4.1.1 Stage 1: optimal rule generation using GSA algorithm

GSA is an optimisation algorithm which is works based on law of gravity. From the above considerations, in this paper we generate an optimal rule and we assume that, which helps to improve the restoration accuracy. Therefore, we make the use of GSA algorithm for selecting optimal rule among n number of rules. The database image D is divided into two sets, training dataset (D_{TR}) and testing dataset (D_{TE}). The training dataset is used to generate the fuzzy rules and based on the rule, we generate the fuzzy system. The accuracy of the proposed system is evaluated with the help of testing images. The detailed process of optimal rule generation using GSA algorithm is explained using the following steps.

Discretisation

After the filtering process, we obtain the distance vector for each window w_{ij}(d_{MFij} and d_{Mij}) which is given to the input of FLS. Here, at first we convert the input vector into particular range which is called discretisation. Discretisation is a process of converting distance vector value into 0 to 1 range. In this paper, we divide the each pixel into maximum intensity value Max_p which is converting the pixel into 0 to 1 range.

$$\hat{Y}_{ij} = \frac{Y_{ij}}{Max_p} \tag{8}$$

Using equation (8), we can adjust all the pixel values in specific interval. Now, we obtain the new values of distance, which values vary from 0 to 1. Then; every value that comes under within the range is replaced with the interval value so that the input data is transformed to the discretised data. Consequently, the input image I is concerted to the discretised format I^D where, the entire pixel value I^D contains only the L, ML, M, and H.

$$\hat{Y}_{ij} = \begin{cases} L & 0 < Y_{ij} < 0.25 \\ ML & 0.25 \le Y_{ij} < 0.5 \\ M & 0.5 \le Y_{ij} < 0.75 \\ H & Y_{ij} \ge 0.75 \end{cases} \tag{9}$$

where Y_{ij} is the i^{th} pixel of the image, L represents the low pixel value, ML represents the moderate low value, M represents the medium value and H is a high pixel value. After the discretisation function, the input image is converted into the discretisation format I^D where, all the element in I^D (i, j) contains only the L, ML, M, H if $K = 4$.

Logical rule generation

Based on the discretised format I^D, we generate the rule; here the rule should have five different decisions such as very low (VL), moderate low (ML), medium (M), moderate high (MH), and very high (VH), respectively. That is, each fuzzy rule contains three linguistic variables, $d_{MF,ij}$, $d_{MN,ij}$ and decision. For $d_{MF,ij}$ and $d_{MN,ij}$, each one has four linguistic terms high distance (H) , moderate low distance (ML), medium distance (M) and low distance (L) while decision has five linguistic terms, VH, MH, M, ML, and VL. These linguistic terms can be expressed by fuzzy sets with the sample rules of the five noise classes are given in Figure 4. The noisy classes are evaluated based on the original image. In this, we compare the fuzzy input linguistic value with original input pixel values. Based on the pixel values, we assign the class for each rule. The repeated rules are removed from the table. The unique rules are used for further process.

Step 1 Solution representation

To optimise the rules, GSA algorithm initially creates arbitrary population of solution. Solution creation is an important step of optimisation algorithm that helps to identify the optimal solution quickly. The dimension of the solution is $1 \times N$. Where, N is the length of the solution. The sample solution format is given in Figure 5. Here, Each Column represents the one rule. The same rule cannot be repeated in the same solution. Here, '0' represents the particular rule which is not selected and '1' represent the particular rule which is selected.

Figure 4 Sample rules

Rule 1: if $d_{MF,ij}$ is H	and	if $d_{MN,ij}$	is	H	Then class is VH
Rule 2: if $d_{MF,ij}$ is H	and	if $d_{MN,ij}$	is	M	Then class is MH
Rule 3: if $d_{MF,ij}$ is H	and	if $d_{MN,ij}$	is	L	Then class is L
Rule 4: if $d_{MF,ij}$ is L	and	if $d_{MN,ij}$	is	L	Then class is VL
Rule n: if $d_{MF,ij}$ is MH	and	if $d_{MN,ij}$	is	H	Then class is M

Figure 5 Solution encoding

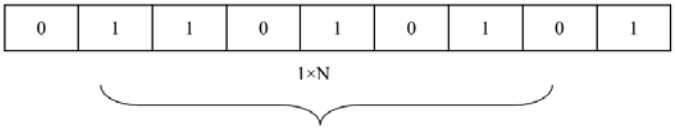

Step 2 Fitness evolution and best fitness computation

After generating the initial solution, the fitness of the solution is evaluated. In this paper, we utilise PSNR as a fitness function.

$$PSNR = 10\log_{10}\left(\frac{255^2}{MSE}\right) \tag{10}$$

$$MSE = \frac{1}{mn}\sum_{i=0}^{m-1}\sum_{j=0}^{n-1}\left[I(i,\ j) - K(i,\ j)\right]^2 \tag{11}$$

where $I(i, j)$ is the original image and $K(i, j)$ is the de-noised image

$$best(t) = \max_{j\in(1,\ldots,N)} Fit_j(t) \tag{12}$$

$$worst(t) = \min_{j\in(1,\ldots N)} Fit_j(t) \tag{13}$$

Step 3 Gravitational constant (G) computation

The gravitational constant G is initialised at the commencement and is scaled down over a period of time so as to manage the search precision. Thus, G represents a function of the initial value G_0 and time (k);

$$G(k) = G_0 e^{-\alpha\frac{k}{T}} \tag{14}$$

where T is the number of iteration, G_0 and α are given constant.

Step 4 Masses of the agent calculation

Gravitational and inertia masses for each agent are calculated at iteration t,

$$M_{ai} = M_{pj} = M_i, \quad \text{where} \quad i = 1, 2, \ldots, N$$

$$m_i(k) = \frac{Fit_i(k) - worst(k)}{best(k) - worst(k)} \tag{15}$$

$$M_i(k) = \frac{m_i(k)}{\sum_{j=1}^{N} m_j(k)} \tag{16}$$

where $Fit_i(k) \rightarrow$ signifies the fitness value of the agent i at time k.

Step 5 Accelerations of agent calculation

Then the acceleration of agent i at time k can be expressed as:

$$A_i(k) = \frac{F_{ij}^d(k)}{M_i(k)} \tag{17}$$

Step 6 Velocity and positions of agents

Moreover, the next velocity of an agent is deemed as a fraction of its current velocity added to its acceleration. Hence, its position and its velocity are evaluated by means of the equations given below.

$$V_i^d(k+1) = rand_i \times V_i^d(k) + A_i(k) \tag{18}$$

$$R_i^d(k+1) = R_i^d(k) + v_i^d(k+1) \tag{19}$$

where $rand_i \rightarrow$ uniform random variable in the interval [0, 1].

Termination criteria

The algorithm stops its implementation only if a maximum number of iterations are attained and the solution, which is containing the best fitness values are chosen and it is given as a best rule to noise detection.

4.1.2 Stage 2: designing of fuzzy system

After the optimal rule generation, we are designing the fuzzy system. When we are designing the fuzzy system, the fuzzy MF definition and fuzzy rule base are the two important steps.

Membership function

A MF is a curve that defines how each point in the input space is mapped to a membership value (or degree of membership) between 0 and 1. Moreover, the MF is designed by choosing the proper MF. Here, we have chosen the triangular MF to convert the input data into the fuzzified value. The triangular MF consists of three vertices *a*, *b* and *c* of *f*(*x*) in a fuzzy set A (a: lower boundary and c: upper boundary where membership degree is zero, b: the centre where membership degree is 1). One of the key issues in all fuzzy sets is how to determine fuzzy MFs,

- the MF fully defines the fuzzy set
- a MF provides a measure of the degree of similarity of an element to a fuzzy set
- MFs can take any form, but there are some common examples that appear in real applications.

The formula used to compute the membership values is depicted as below,

$$f(x) = \begin{cases} 0 & \text{if } x \le a \\ \dfrac{x-a}{b-a} & \text{if } a \le x \le b \\ \dfrac{c-x}{c-b} & \text{if } b \le x \le c \\ 0 & \text{if } x \ge c \end{cases} \tag{20}$$

Rule-based fuzzy score computation

Using GSA optimisation algorithm, we already generated the fuzzy rule set in Figure 4. These rules are given to the FL. The rule base contains a set of fuzzy rule in the form of, low, high, moderate and medium distance values. After the fuzzification process the fuzzy classifier generate the score value F^{score}. Depends upon the score value, we can detect the present pixel is corrupted or not. Here, we used one threshold (T_h) value for detect the error. If the score value is above the threshold means the pixel corrupted otherwise the pixel is noise free. Thus the obtained score value is assessed with the condition (21) which is given in below for the purpose of detecting the noise pixel. If the pixel is corrupted means, we again apply the MF to corrupted pixel and restore the image. Finally, we obtain the restored image $O(i, j)$.

$$result = \begin{cases} T_h \ge \text{score ; pixel is noise free} \\ T_h < \text{score ; pixel is noise} \end{cases} \tag{21}$$

Table 1 Pseudo code of proposed image restoration

```
Input:
Input image I(i, j)
        Parameter of GSA algorithm
Output: restored image O(i, j)
Start:
1. Get the input image I(i, j)
2. Add the impulse noise to the I(i, j)
3. Split the image I(i, j) into 3 × 3 window w_ij
4. Then for each window
   {
      apply median filter …… refer section 3
      Apply mean filter ……. refer section 3
   }
```

Table 1 Pseudo code of proposed image restoration (continued)

5. end for
6. then calculate the distance between centre pixel Y_{ij} and $Y_{MF,ij}$, $Y_{MN,ij}$
7. Finally obtain the distance vector $d_{MF,ij}$, and $d_{MN,ij}$
8. design the fuzzy system based on $d_{MF,ij}$, and $d_{MN,ij}$
9. apply the discretisation process using equations (8) and (10)
10. generate the rule
11. select the optimal rule using GSA

{

Generate the initial population of GSA (refer Figure 5)

Calculate the fitness value using equation (10)

}

Repeat

{

12. compute the gravitational constant using equation (14)
13. compute Masses of the agents' calculation using equation (16)
14. calculate acceleration of agent's using equation (17)
15. update agent's velocity and position using equations (18) and (19)

}

16. repeat
17. Stop the criteria if the optimal rule is obtained
18. Select the optimal rule
19. Given the optimal rule to fuzzy logic system
20. estimate rule-based score value
21. After the fuzzy logic system, detect particular pixel is corrupted or not using equation (21)
22. if pixel is corrupted

{ apply the median filter

}

End if

23. finally obtain the restored the image $O(i, j)$
24. end

5 Result and discussion

In this section, the proposed image restoration process discussed in the previous section is implemented. In this paper, we used standard test images for the image restoration process. The proposed image restoration technique has been implemented in the working platform of MATLAB (version7. 12). This technique is performed on a windows machine having configuration processor® Dual-core CPU, RAM: 1 GB, Speed: 2.70 GHz with Microsoft Window7 professional operating system. We have utilised the size

of the image '512 × 512', whose images are publicly available. Figure 6 shows the some of the sample images used in experimentation.

Figure 6 Sample images

5.1 Evaluation metrics

The evaluation of proposed image restoration technique is carried out using the following metrics as suggested by below.

- *PSNR:* the peak signal to noise ratio (PSNR) is used to measure the quality of the output restored image. The PSNR is the ratio between the input image and restored image. The PSNR is identified using the mean square error (MSE). The MSE gives the cumulative squared error between the corrupting noise and the maximum power of the signal. Higher the PSNR and lower the MSE, better the de-noised image.

$$PSNR = 10\log_{10}\left(\frac{255^2}{MSE}\right)$$

$$MSE = \frac{1}{M * N}\sum_{i=1}^{M}\sum_{j=1}^{N}\left[I(i,\ j) - O(i,\ j)\right]^2$$

where

$I(i, j)$ input image

$O(i, j)$ de-noised image.

5.2 Experimental results

The main objective of this paper is to image restoration using a combination of optimal FLS and multiple filters. Here, at first we split the input image into number of windows. Then each window, we apply the multiple filters such as MF and mean filter. After filtering process, we calculate the distance vector based on original window and filtered window. Then, this distance vector is given to the input of the optimal FLS. After that, based on the distance vector the FLS generate the rule. Large number of rules is great

obstacle of noise pixel detection. Therefore, in this work we optimise the using GSA. Finally, we detect the noise pixel and restore using MF. The experimental results of proposed image restoration are given in Figure 7.

Figure 7 Experimental results of proposed image restoration approach, (a) input image (b) noisy image (c) restored image

(a) (b) (c)

The basic idea of our research is to restore the image using optimal FLS with a multiple filter. The experimental results of proposed restoration output are given in Figure 5. In this paper, we used five types of standard test images for experimentation. Here, we added the 20, 40, 60, 80 and 100%impulse noise. Moreover, Figure 8 shows the fitness plot for GAS and GA. In this paper, the optimal FL rules are selected using GSA

algorithm. GSA algorithm works based on the law of gravity. From Figure 8, we clearly understand our proposed GSA-based fitness function is better than GA.

Figure 8 Fitness plot for GSA and GA (see online version for colours)

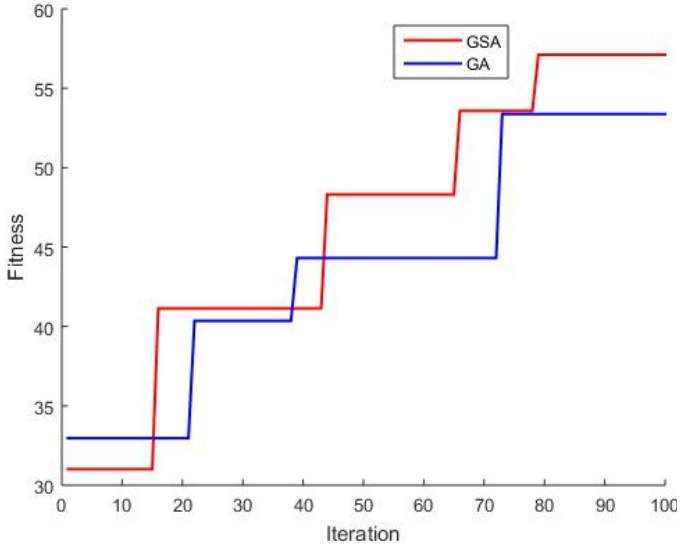

5.3 *Comparative analysis of proposed methodology*

To evaluate the performance of our proposed approach, we compare our results with other methods. Here, we compare our proposed work (GSA + FLS) with four other approaches such as GA+FLS, FLS, based image restoration approaches. The GA + FLS method utilised the GA algorithm for rule optimisation and FLS for the noise detection process (Stefan et al., 2007). This method is same as our proposed algorithm, only the difference is optimisation algorithm. Using the GA, we cannot get maximum PSNR because GA has no guarantee of finding global maxima and this algorithm takes maximum time for convergence. Avoiding this problem, in this paper we proposed the GSA. Moreover, we compare our proposed work with another approach which is FLS. Using FLS approach, the author did not use any optimisation algorithm. Here, the whole rules are directly given to the FLS.

Table 2 PSNR measure for different images by adding 20% of impulse noise

Image name	*PSNR*				
	GA + FLS	*FLS*	*GSA + FLS*	*Mean filter*	*Median filter*
Baboon	59.27704	57.586	59.82653	56.61304	57.98236
Barbara	61.96303	60.35262	62.13103	56.9533	59.71856
Cameraman	62.01236	60.69631	62.62393	56.91979	59.76206
House	63.55444	61.62601	64.38662	56.88681	58.98864
Lena	62.39437	61.56271	63.11792	57.92648	59.36137

Table 3 MSE measure for different images by adding 20% of impulse noise

Image name	*MSE*				
	GA + FLS	*FLS*	*GSA + FLS*	*Mean filter*	*Median filter*
Baboon	0.096803	0.113365	0.075933	0.141833	0.103477
Barbara	0.071379	0.099954	0.039809	0.131145	0.169378
Cameraman	0.067312	0.075392	0.037212	0.13216	0.15456
House	0.072784	0.07552	0.023682	0.133168	0.141135
Lena	0.059761	0.085374	0.031717	0.104817	0.147527

Table 4 PSNR measure for different images by adding 40% of impulse noise

Image name	*PSNR*				
	GA + FLS	*FLS*	*GSA + FLS*	*Mean filter*	*Median filter*
Baboon	57.357	56.142	58.312	53.94	55.35
Barbara	60.463	58.682	61.105	55.534	56.1534
Cameraman	61.275	59.164	61.572	55.363	56.465
House	62.168	60.01	63.421	54.231	56.964
Lena	61.054	59.270	62.643	56.453	57.361

Table 5 MSE measure for different images by adding 40% of impulse noise

Image name	*MSE*				
	GA + FLS	*FLS*	*GSA + FLS*	*Mean filter*	*Median filter*
Baboon	0.1252	0.143365	0.0835	0.1761	0.1543
Barbara	0.141	0.1734	0.0464	0.1935	0.1834
Cameraman	0.1326	0.1552	0.04821	0.1832	0.1632
House	0.1486	0.1502	0.03912	0.17834	0.1675
Lena	0.15753	0.1634	0.0475	0.1932	0.1846

Table 6 PSNR measure for different images by adding 60% of impulse noise

Image name	*PSNR*				
	GA + FLS	*FLS*	*GSA + FLS*	*Mean filter*	*Median filter*
Baboon	57.01	55.99	58.14	53.43	55.04
Barbara	59.352	58.361	60.95	55.24	55.94
Cameraman	61.032	59.01	61.352	55.12	56.231
House	61.54	59.94	63.232	53.93	56.436
Lena	60.921	59.10	62.312	56.241	57.271

Table 7 MSE measure for different images by adding 60% of impulse noise

Image name	*MSE*				
	GA + FLS	*FLS*	*GSA + FLS*	*Mean filter*	*Median filter*
Baboon	0.1252	0.143365	0.0835	0.1761	0.1543
Barbara	0.141	0.1734	0.0464	0.1935	0.1834
Cameraman	0.1326	0.1552	0.04821	0.1832	0.1632
House	0.1486	0.1502	0.03912	0.17834	0.1675
Lena	0.15753	0.1634	0.0475	0.1932	0.1846

Table 8 PSNR measure for different images by adding 80% of impulse noise

Image name	*PSNR*				
	GA + FLS	*FLS*	*GSA + FLS*	*Mean filter*	*Median filter*
Baboon	56.94	55.54	57.98	53.10	54.78
Barbara	59.132	58.103	60.45	54.94	55.16
Cameraman	60.943	58.84	61.01	54.94	56.02
House	61.20	59.36	62.92	53.36	56.25
Lena	60.352	58.94	62.143	55.94	57.102

Table 9 MSE measure for different images by adding 80% of impulse noise

Image name	*MSE*				
	GA + FLS	*FLS*	*GSA + FLS*	*Mean filter*	*Median filter*
Baboon	0.152	0.193	0.0895	0.192	0.1834
Barbara	0.172	0.1934	0.0531	0.231	0.1943
Cameraman	0.162	0.1932	0.0499	0.2043	0.1934
House	0.1823	0.1943	0.0445	0.1943	0.1932
Lena	0.1831	0.1753	0.0512	0.2054	0.1932

Table 10 PSNR measure for different images by adding 100% of impulse noise

Image name	*PSNR*				
	GA + FLS	*FLS*	*GSA + FLS*	*Mean filter*	*Median filter*
Baboon	56.32	55.32	57.43	52.74	54.24
Barbara	58.54	57.54	60.12	54.52	55.01
Cameraman	60.35	58.367	60.54	54.43	55.43
House	60.85	59.12	62.43	53.312	56.01
Lena	60.14	58.32	62.01	55.42	56.45

Table 11 MSE measure for different images by adding 100% of impulse noise

Image name	*MSE*				
	GA + FLS	*FLS*	*GSA + FLS*	*Mean filter*	*Median filter*
Baboon	0.143	0.23	0.092	0.23	0.192
Barbara	0.163	0.214	0.0832	0.253	0.2254
Cameraman	0.171	0.251	0.021	0.247	0.201
House	0.19	0.244	0.082	0.243	0.230
Lena	0.192	0.194	0.073	0.251	0.251

Table 2 shows the performance of PSNR measure for different images by adding 20% of impulse noise. When analysing Table 2, our proposed approach achieves the maximum PSNR of 64.38662 db for house image which is 62.95066 db for using GA+FLS, 60.69 db for using FLS, 57.92648 db for using MF and 59.76206 db for using MF-based image restoration. Individual MF and mean filters achieves the poor performance compare to GA+FLS, FLS and GSA+FLS-based image restoration. To improve the performance of

the proposed system, we used multiple filters. Similarly, Table 3 shows the performance of MSE measure for different images by adding 20% of impulse noise. Here, our proposed approach achieves the minimum MSE of 0.023682 for house image. Table 4 shows the performance of PSNR measure for different images by adding 40% of impulse noise. When analysing Table 4, our proposed approach achieve the maximum PSNR of 58.312db for using Baboon image, 61.105 db for using Barbara image, 61.572 db for using Cameraman image, 63.421db for using house image and 62.643 for using Lena image. Similarly, Table 5 shows the performance of MSE measure for different images by adding 40% impulse noise. Here, our proposed approach achieves the minimum MSE. Additionally, Table 6 shows the PSNR measure for different images by adding 60% of impulse noise. Here, our proposed approach achieves the maximum PSNR of 61.352 db which is 59.94 db for using FLS-based image restoration, 61.54 db for using GA + FLS-based image restoration, 56.241db for using Mean filter-based image restoration, 57.271db for using MF-based image restoration. Similarly, Table 7 shows the performance of MSE measure for different images by adding 60% of impulse noise. When analysing Table 7, our proposed approach obtain the minimum error compare to other approaches. Moreover, Table 8 shows the performance of PSNR measure for different images by adding 80% of impulse noise. When analysing Table 8, our proposed approach achieves the maximum PSNR of 62.92db which is 59.36 db for using FLS-based image restoration, 60.943db for using GA+FLS-based image restoration, 55.94 for using Mean filter-based image restoration, 57.102 db for using MF-based image restoration. Similarly, Table 9 shows the Performance of MSE measure for different images by adding 80% of impulse noise. Compare to other work, our proposed image restoration achieves the minimum error rate. Theperformance of PSNR measure for different images by adding 100% of impulse noise. Here, our proposed approach achieves the maximum PSNR of 57.43 db for baboon image, 60.12 for Barbara image, 60.54 for cameraman image, 62.43 for house image and 62.01 db for Lena image. From Table 10, we clearly understand our proposed approach achieves the maximum PSNR compare to other approaches. Similarly, Table 11 shows the performance of PMSE measure for different images by adding 100% of impulse noise. The noise level increase means the MSE also increases. From the, experimental results, we clearly understand our proposed approach achieves the maximum PSNR and minimum MSE compare to other approaches.

6 Conclusions

This paper has proposed image restoration using multiple filters with optimal FLS. The proposed image restoration, at first splits the input image into number of windows. Subsequently, we apply the multiple filters to each window which is design an impulse ND for test images and also at the same time utilises the FLS and the GSA algorithm to realise the ND. Two image de-noising filters, the MF, and the MNF have been finely employed to design the input of the FLS which can successfully judge the impulse noises and attain enhanced performance in noise detection. To enhance the proposed methodology, GSA algorithm is used to select the optimal rule and the selected rules are given to the FLS. Finally, if the pixel is noise corrupted means, we can remove the noise using MF. The proposed method is able to perform a very strong noise cancellation compared with other approaches. The experimental results are demonstrated our

approach achieves the maximum PSNR of 64.38662 which is high compared to existing approaches. In future, I will explain this work with some other filters and will be utilise hybrid optimisation algorithm for rule generation.

References

Adjeroh, D.A., Zhang, Y. and Parthe, R. (2006) 'On denoising and compression of DNA micro array images', *Journal of Pattern Recognition*, Vol. 39, No. 12, pp.2478–2493.

Arridge, S.R. (1999) 'Optical tomography in medical imaging', *Inverse Problems*, Vol. 15, No. 2, pp.41–93.

Cai, J.F., Dong, B. and Shen, Z. (2006) 'Image restoration: a wavelet frame based model for piecewise smooth functions and beyond', *Applied and Computational Harmonic Analysis*, Vol. 41, No. 1, pp.94–138.

Chan, T., Esedoglu, S., Park, F. and Yip, A. (2005) 'Recent developments in total variation image restoration', *Mathematical Models of Computer Vision*, pp.1–18, Springer, New York.

Chen, Y., Zhang, Y. and Zhang, K. (2016) 'FIRT: filtered iterative reconstruction technique with information restoration', *Journal of Structural Biology*, Vol. 195, No. 1, pp.49–61.

Guerrero-Colon, J.A., Mancera, L. and Portilla, J. (2007) 'Image restoration using space-variant Gaussian scale mixtures in over complete pyramids', *IEEE Trans. Image Process.*, Vol. 17, No. 1, pp.27–41.

Johnson, C. and Sofer, A. (2000) 'A primal-dual method for large-scale image reconstruction in emission tomography', *SIAM Journal on Optimization*, Vol. 11, No. 3, pp.691–715.

Kaipio, J., Kolehmainen, V. and Somersalo, E. (2000) 'Statistical inversion and Monte Carlo sampling methods in electrical impedance tomography', *Inverse Problems*, Vol. 16, No. 5, pp.1487–1522.

Ketter, E. (2016) 'Destination image restoration on Facebook: the case study of Nepal's Gurkha earthquake', *Journal of Hospitality and Tourism Management*, Vol. 28, pp.66–72.

Laghrib, A., Ghazdali, A. and Hakim A. (2016) 'A multi-frame super-resolution using diffusion registration and a nonlocal variational image restoration', *Computers & Mathematics with Applications*, Vol. 72, No. 9, pp.2535–2548.

Li, L., Wang, J. and Lu, W. (2016) 'Simultaneous tumor segmentation, image restoration, and blur kernel estimation in PET using multiple regularizations', *Computer Vision and Image Understanding*, Vol. 55, pp.173–194.

Li, Y. and Santosa, F. (1996) 'A computational algorithm for minimizing total variation in image restoration', *IEEE Transactions on Image Processing*, Vol. 5, No. 6, pp.987–995.

Liu, S., Wu, G. and Liu, H. (2016) 'Image restoration approach using a joint sparse representation in 3D-transform domain', *Digital Signal Processing*, Vol. 60, pp.307–323.

Lukac, R. and Plataniotis, K. N. (2007) 'Vector edge operators for cDNA microarray spot localization', *Journal of Computer Medical Imaging Graph*, Vol. 31, No. 7, pp.510–522.

Lukac, R. and Smolka, B. (2003) 'Application of the adaptive center-weighted vector median framework for the enhancement of cDNA microarray images', *International Journal of Applied Mathematics and Computer Science*, Vol. 13, No. 3, pp.369–383.

Majava, K. (2001) 'Optimization-based techniques for image restoration', *Jyvaskyl a Studies in Computing*, No. 14.

Mbarki, Z., Seddik, H. and Braiek, E.B. (2016) 'A rapid hybrid algorithm for image restoration combining parametric wiener filtering and wave atom transform', *Journal of Visual Communication and Image Representation*, Vol. 40, pp.694–707.

Mei, J.J. and Huang, T.Z. (2016) 'Primal-dual splitting method for high-order model with application to image restoration', *Applied Mathematical Modelling*, Vol. 40, No. 3, pp.2322–2332.

Mignotte, M. (2005) 'An adaptive segmentation-based regularization term for image restoration', *Proc. IEEE Int. Conf. Image Process.*, Vol. 1, pp.901–904.

Molina, R., Mateos, J. and Katsaggelos, A. K. (2006) 'Blind deconvolution using a variational approach to parameter image, and blur estimation', *IEEE Transactions on Image Processing*, Vol. 12, No. 12, pp.3715–3727.

Portilla, J. and Simoncelli, E.P. (2003) 'Image restoration using Gaussian scale mixtures in the wavelet domain', *Proc. IEEE Int. Conf. Image Process.*, Vol. 2, pp.965–968.

Rao, D.H. (2006) 'A survey on image enhancement techniques: classical spacial filter', *IEEE International Conference on Neural Network, Cellular Neural Network, Fuzzy Filter. Industrial Technology, ICIT 2006*, pp.2821–2826.

Sakthidasan, K. and Nagappanb, N.V. (2016) 'Noise free image restoration using hybrid filter with adaptive genetic algorithm', *Computers & Electrical Engineering*, Vol. 54, pp.382–392.

Senthilselvi, A. and Sukumar, R. (2014) 'A survey on image restoration technique', *International Journal of Emerging Engineering Research and Technology*, Vol. 2, No. 8, pp.123–128.

Senthilselvi, A. and Sukumar, R. (2018) 'Removal of salt and pepper noise from images using hybrid filter (HF) and fuzzy logic noise detector (FLND)', *Journal of Concurrency and Computation: Practice and Experience* [online] http://dx.doi.org/10.1002/cpe.4501.

Shi, M., Han, T. and Liu, S. (2016) 'Total variation image restoration using hyper-Laplacian prior with overlapping group sparsity', *Signal Processing*, Vol. 126, pp.65–76.

Stefan, S., De Witte, V., Nachtegael, M., Van der Weken, D. and Kerre, E.E. (2007) 'Histogram-based fuzzy colour filter for image restoration', *Journal of Image and Vision Computing*, Vol. 25, No. 9, pp.1377–1390.

Zhao, J.F and Feng, H. J. (2012) 'An improved image restoration approach using adaptive local constraint', *Opt. Int. J. Light. Electron. Opt.*, Vol. 123, No. 11, pp.982–985.